THE EFFECT OF NON-NEWTONIAN FLOW BEHAVIOUR ON BINARY DROPLET COLLISIONS: VOF-SIMULATION AND EXPERIMENTAL ANALYSIS

M. Motzigemba[a], N. Roth[b], D. Bothe[a], H.-J. Warnecke[a], J. Prüss[c], K. Wielage[d], B. Weigand[b]
mmotz1@tc.uni-paderborn.de
[a]Chemical Engineering, University of Paderborn, 33095 Paderborn, Germany
[b]Institute of Aerospace Thermodynamics (ITLR), University of Stuttgart, Stuttgart, Germany
[c]Institute of Analysis, Martin Luther University Halle-Wittenberg, Halle, Germany
[d]Paderborn Center for Parallel Computing PC², University of Paderborn, Paderborn, Germany

Abstract
Experimental investigations and numerical simulations of binary droplet collisions using Newtonian and non-Newtonian fluids have been performed. This provides a validation of the employed numerical methods and simulation software as well as a first insight into the basic phenomenon of binary droplet collision with non-Newtonian fluids.
The Newtonian, respectively non-Newtonian fluids used were glycerol/water and shear-thinning water/carboxymethylcellulose (CMC). The non-Newtonian behaviour was modelled by means of a generalized Newtonian constitutive equation using a modified power law viscosity function.
A shear-thinning liquid shows its lowered viscosity during the droplets collision by a larger maximum diameter of the generated collision complex, compared to a Newtonian collision with similar values of the characteristic dimensionless groups. This behaviour can be simulated and quantitatively reproduced by the three-dimensional CFD code FS3D (University of Stuttgart, ITLR), which has been extended in the present investigation towards non-Newtonian fluids. The code uses the Volume-of-Fluid (VOF) method for the description of the free fluid surface. The obtained results increase confidence in the selected generalized Newtonian modelling for the experimental fluid.
The dimensionless time until the collision complex attains its maximum expansion is found to be independent of the viscosity characteristics; it is only a function of the Weber number. Therefore, the absolute time for reaching the maximum complex diameter for a given Weber number is merely proportional to the ratio of droplet diameter to droplet velocity.
The simulated velocity fields show that at all stages of the collision process there are areas in which the velocity gradients for shear are larger than the elongational ones, and vice versa. Overall, elongational flow dominates.

Introduction

Droplet collisions are of importance in a variety of practical applications comprising disperse two-phase flow. In applications dealing with polymers, non-Newtonian rheological behaviour comes into focus. One application of special interest to our research is the disintegration of polymer melts for powder coatings production.

This work reports on results obtained from both experimental and numerical studies of binary droplet collisions in air of a Newtonian and a non-Newtonian fluid with pseudoplastic shear behaviour (obeying a modified power law). The non-Newtonian fluid was selected regarding two criteria: high shear-thinning effect and low elastic effects. Its flow behaviour is assumed to be that of a generalized Newtonian fluid.

Experimental Investigation

The Newtonian and the Non-Newtonian Test Liquid: Viscosity

The Newtonian liquid used was an 84 wt% aqueous solution of glycerol, obtained by mixing demineralised water with glycerol (Glycerin Ph Eur). The viscosity at 20.0 °C was 100 mPas.

The non-Newtonian liquid was an aqueous polymer solution containing 2.8 wt% carboxymethylcellulose sodium salt (CMC, Walocel Crt 20 Ga) provided by Wolff Walsrode. It was prepared by adding the solid CMC to demineralised water contained in a well-stirred tank during an empirically defined period of time. Data of its measured shear viscosity are shown in figure 1. The measurements were done by rotary viscometry. For the highest shear rates reached by this method, the fluid showed no region of constant viscosity.

Figure 1 shows also a best-fit curve of a modified power law modelling, using a viscosity function of type

$$\mu = \frac{\mu_0}{1 + \frac{\mu_0}{K}\dot{\gamma}^{1-n}} \qquad (1)$$

The fluid was chosen for low elastic effects, but still significant effect of shear on viscosity. Thereby the applicability of the generalized Newtonian model (see section Numerical Simulation below) is optimised while retaining unambiguous experimental results.

Experimental Procedure

The droplet collisions were realized by means of two crossing monodisperse coherent droplet streams produced by two piezoelectrically-excited droplet stream generators [1,2]. Droplets are generated by liquid flow through a circular orifice and subsequent Raleigh break-up of the produced jet. The experimental set-up was designed for low viscosity liquids (propanol, ethanol) but worked also for the higher viscosity fluids used here.

The experimental equipment comprises the nozzles for generating the two droplet streams, whose point of intersection is viewed from two cameras positioned co-planar or perpendicular to the plane of streams. The droplet collision area is illuminated by a flash lamp, whose light is split by a beam splitter and reflected by two mirrors yielding light parallel to the optical axes of the viewing cameras. The cameras are connected to a video mixer and a video recorder.

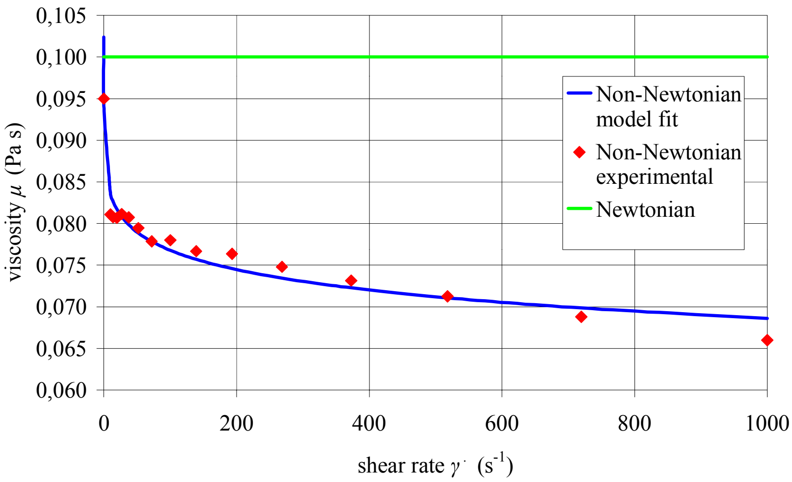

Figure 1. Viscosity of the experimental liquids: experimental values and fit-curve for the modified power-law model.

For the results presented in this paper, the diameters of the droplets before impact were varied from 0.3 to 0.7 mm.

The measurements of the diameters were based on the photographs from the video recordings (e.g. figure 2). Diameters were measured using an image analysis software. The definition of a light intensity threshold for the boundary detection is therefore necessary. The range of diameters for the possible threshold range quantifies the uncertainties of the measurements. We obtained uncertainties of +/- 10 % based on the single-drop diameter.

Experimental Results: the Effect of Shear-Thinning on Droplet Collision

The droplet-droplet collisions for Newtonian and shear–thinning fluid are shown in figure 2 using the combined images from both cameras. Figure 3 shows the evolution of the dimensionless diameter *d/D*. Here Newtonian and non-Newtonian cases with $\mu_N = \mu_0$ are contrasted for various Weber and Reynolds numbers. From this figure, it can be seen that the maximum of the diameter function increases with increasing *We*.

Besides the first maximum of the complex diameter, one can see a small oscillation of the diameter function

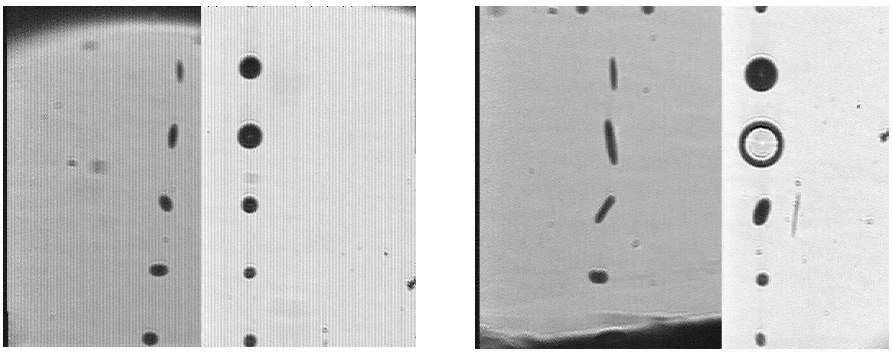

(a) (b)

Figure 2. Binary droplet collisions for 120 μm droplet diameter with different fluids and similar flow: (a) Newtonian, *We* = 657, *Re* = 55; (b) Non-Newtonian, *We* = 766, *Re* = 49.

for larger t^*. The amplitude of this oscillation is always larger for the shear thinning case compared to the Newtonian case with similar Weber number. The influence of flow characteristic on the maximum dimensionless diameter is extracted in figure 4. The dependency of the maximum diameter on *We* (and *Re*) shows the enlarging influence of inertia forces. Here one can also see the significant effect of the non-Newtonian behaviour: the non-Newtonian complexes show much larger diameters than the Newtonian ones.

Figure 3 also gives information about the time-scale of the droplet collision expansion. The time for maximum expansion of the collision complex shows a strictly monotonic dependency on the Weber number but seems to be independent from the nature of the viscosity function.

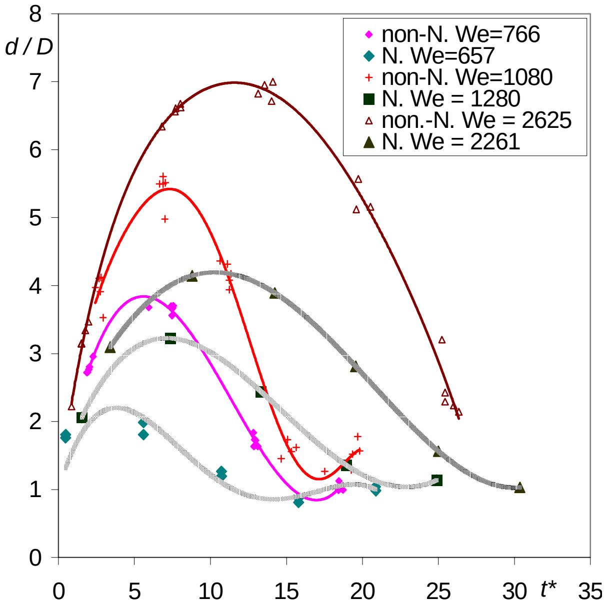

Figure 3. Dimensionless diameter of collision complex vs. dimensionless time $t^*=t/(D/U)$ at various velocities, expressed by *We*, for Newtonian (thick lines) or non-Newtonian (thin lines) liquids.

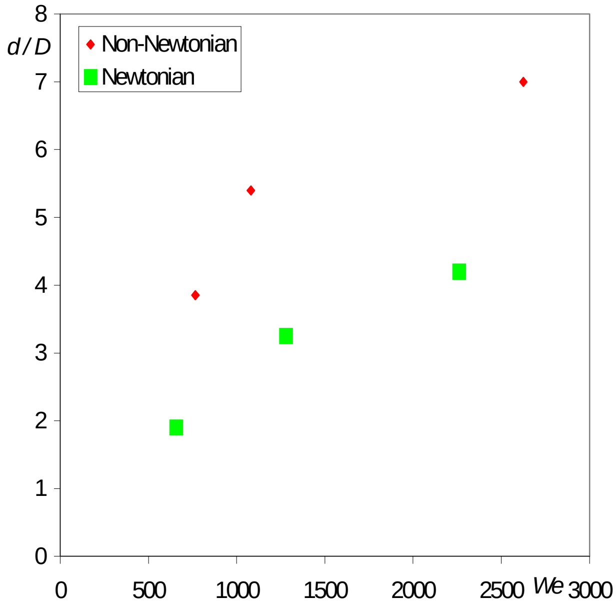

Figure 4. Maximum dimensionless diameter of collision complex versus *We* for Newtonian and non-Newtonian liquids.

Numerical Simulation

Mathematical Modelling

Collision of liquid droplets in air can be described as an incompressible transient two-phase flow. The modelling is based on continuum mechanics using the transport equations for mass and momentum, where the particular material behaviour is incorporated by a constitutive equation for the deviatoric stress tensor. By the Volume-of-Fluid (VOF) method, an additional transport equation for the volume fraction of one of the phases is introduced [3,4]. It further involves treatment of the interface tension forces by an additional term in the momentum equations.

To investigate the influence of one type of non-Newtonian behaviour on the results, the constitutive equation of the generalized Newtonian fluid was chosen (e.g. [5]). The deviatoric stress tensor is defined by

$$\tau(\mu,u)=\mu(\dot{\gamma})\cdot\left[(\nabla u)+(\nabla u)^T\right] \tag{2}$$

The non-Newtonian fluid used in the experiments is considered to obey such a generalized Newtonian fluid constitutive equation. Its elongational viscosity is therefore $\bar{\mu}=3\mu$. Experimental measurements of elongational viscosity were not done so far. The selected viscosity function μ is the modified power law equation (1) extended from one-dimensional pure-shear flow to an arbitrary three-dimensional flow:

$$\mu=\frac{\mu_0}{1+\frac{\mu_0}{K}\dot{\gamma}^{1-n}} \qquad \text{with } \dot{\gamma}=\sqrt{\frac{1}{2}\sum_{i,j}\left(\frac{\partial u_i}{\partial x_j}+\frac{\partial u_j}{\partial x_i}\right)^2}\,. \tag{3}$$

For the simulation, a parallel CFD code (FS3D, University of Stuttgart, ITLR) has been used. It is based on a three-dimensional Finite-Volume approach and uses the Volume-of-Fluid (VOF) method. The involved treatment of the interface tension is based on a conservative approximation described by Lafaurie *et. al*. [6].

Simulations have been performed in three dimensions with or without symmetry planes. Three-dimensional simulations had to be used in order to ensure the correct values for shear rate and surface curvature.

When symmetry planes are used, the two colliding droplets are represented by one quarter of a droplet – using symmetry planes xz and yz – moving along the z-axis towards the origin, thereby colliding with its mirror image, created by the third symmetry plane xy.

Verification of the Code for Non-Newtonian Flows

The code *FS3D* has previously been validated for Newtonian two-phase flow by means of comparison with experimental results from several droplet collision or impact experiments. As a first step, the extension of the code towards the calculation of non-Newtonian fluid behaviour had to be verified. For the chosen type of viscosity function (3), an analytical solution of the governing equations can be found for simple single-phase flow problems. A single-phase steady laminar flow between two stationary parallel planes of infinite extent was chosen as an appropriate problem. For material parameter n = 0.5 an analytical solution can be derived:

$$v(y) = \begin{cases} \frac{1}{48a^4b^2}\left[a^6 d_P^3 + 2a^3b^2 d_P c + a^4 b d_P^2 (6+ac)\right] + \frac{1}{6a^4b^2}\left[-3a^4 b y^2 + a^6 y^3 + \left(6ab^3 + a^3b^2 y - a^5 b y^2\right) f(y)\right] & \\ + \frac{1}{6a^4b^2}\left\{12b^3\left[\log\left(\frac{-2b + a^2 y + ab\, f(y)}{ab}\right) - \log\left(2\left(-\frac{4}{a} - \frac{a d_P}{b} + c\right)\right)\right] - 3ab^3 c\right\} & \text{if} \quad \frac{-d_P}{2} \le y \le 0 \\ v(-y) \qquad \text{if} \quad 0 < y \le \frac{d_P}{2}; & \end{cases} \tag{4}$$

$$a = \frac{\mu_0}{K},\ b = \mu_0 \frac{L}{\Delta P},\ c = \sqrt{\frac{d_P(8b + a^2 d_P)}{b^2}},\ f(y) = \sqrt{\frac{y\left(-4b + a^2 y\right)}{b^2}}$$

The simulation of this channel flow was done for flow parameters similar to the droplet collision flow. To quantify the similarity of the two flows, a modified Reynolds number Re_M was introduced. The required value of $\dot{\gamma}$ for the droplet collision flow was obtained from the simulations as the maximum simulated value of $\dot{\gamma}$.

The numerical solution agrees well with the analytical one. The maximum error of velocity is below 1 %.

Computational Results: Comparison with Experiment and Evolution of Viscosity—Velocity Fields

Experimental imaging and simulation of the droplet-droplet collisions for the shear–thinning fluid are shown in figure 5. It reveals that the surface shape can be reproduced by the simulation. Figure 6 shows the evolution of the dimensionless diameter *d/D*. Here experimental

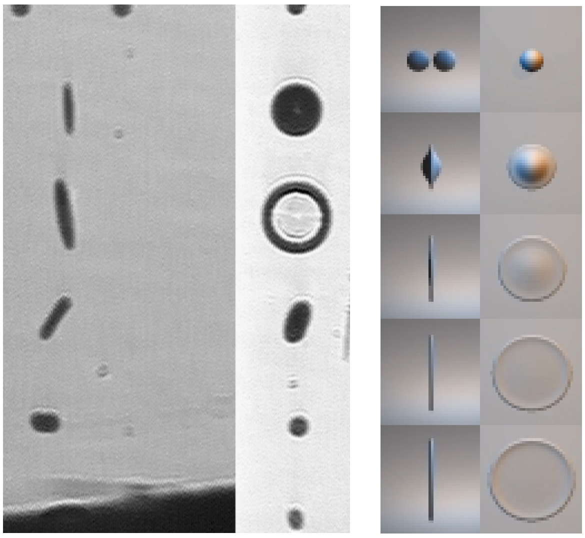

(a) (b)

Figure 5. Shape of collision complex for the non-Newtonian liquid, (a) experiment, (b) simulation.

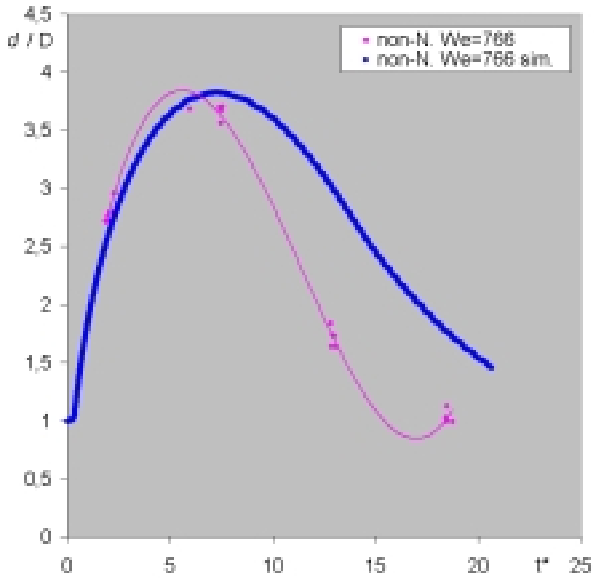

Figure 6. Dimensionless diameter of collision complex vs. dimensionless time *t*=t/(D/U)* for non-Newtonian liquid: experiment and simulation.

and numerical data are shown for one set of flow and material parameters. A good agreement between the dimensionless diameter *d/D* obtained from the simulations and the experiments is found for the expansion of the collision complex. The deviation of maximum collision complex diameter is below 4 %. For the subsequent contraction the simulated times for an equivalent collision complex shape are overestimated.

Despite the good quantitative results for collision complex diameter, problems were encountered for computing the surface of the thin inner lamella of the collision complex. The thickness of the lamella reaches the order of one cell size. Therefore, the volume fraction may fall below 1. Since the surface tension modelling of the VOF Code is based on a volume fraction jump from 0 to 1 across the gas/liquid interface, disturbed values for volume forces and surface normal vector will be calculated. The problem is exacerbated by the occurrence of entrapped air bubbles within the lamella in the numerical simulation. These bubbles do not occur visibly in the experiments. They further reduce the lamella thickness from the inside. The positions of these bubbles are the starting points of the simulated lamella break-up shortly after maximum expansion of the collision complex; this could not be observed in the experiments.

The simulation gives further insight into the collision phenomenon. The evolution of viscosity during different stages of the collision is shown in figure 7. The viscosity is significantly lowered throughout the whole collision complex, never reaching the zero shear viscosity of 102 mPas. The minimum of viscosity occurs at the moment of droplet impact at the impact location due to a peak of (elongational) shear rate. At the beginning, there is a gradient of viscosity along the collision axis (z-direction), giving values from 45 mPas at impact location to 80 mPas at the opposite side. The gradient and the range of viscosity decrease during collision complex evolution, but do not vanish.

Furthermore, the numerical results give some information about the nature of this droplet collision flow in terms of shear or elongational flow. Figure 8 shows the velocity field in z- and y-direction shortly after contact. The dominance of the gradients of the shown velocity fields in or perpendicular to the flow component direction give information about the prevailing flow, elongational or shear respectively. Depending on position both types of flow are encountered. This is also the case for later stages of the collision process.

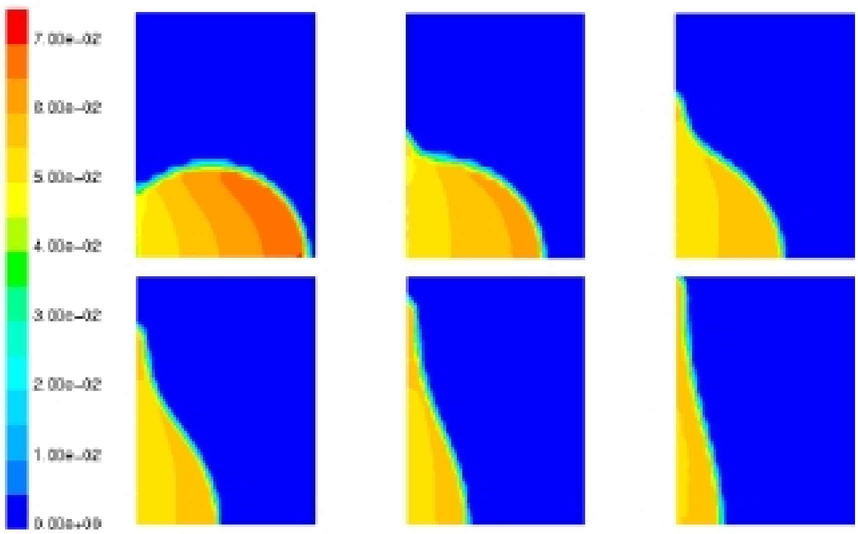

Figure 7. A quarter of a droplet of the non-Newtonian fluid moves to the left towards the origin and collides with its mirror image, realized by a mirror plane on the left. The viscosity μ (in Pas) at different stages of the collision is visualized in a contour plot.

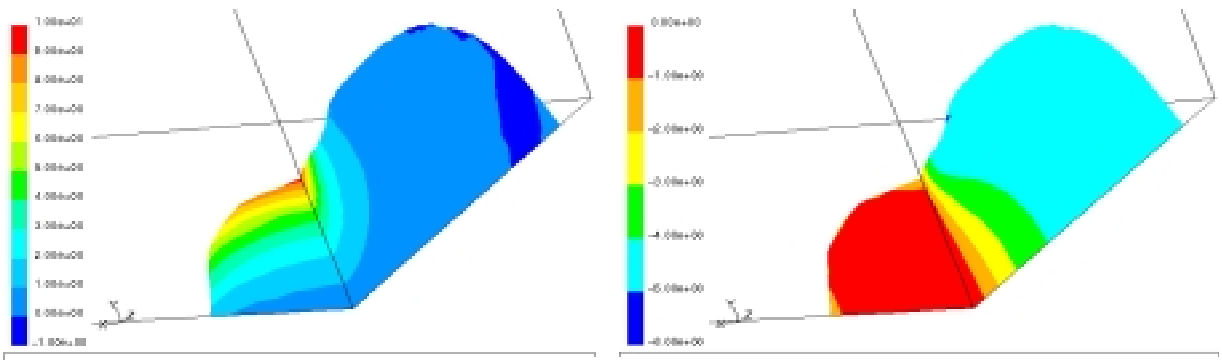

(a) (b)

Figure 8. A quarter of a droplet of the non-Newtonian fluid moves along the z-axis towards the origin and collides with the mirror plane xy. Visualised are (a) y-velocity and (b) z-velocity. The time is $t^* = 0.36$. The ratio of the gradients of the shown velocities determines the prevailing flow: shear or elongational.

Discussion and Conclusions

Simulations performed for a generalized Newtonian fluid showed manifestations of shear thinning by the enlargement of the collision complex compared to the Newtonian case for the same Weber numbers. The same effect was found in the experimental comparison of the shear-thinning CMC-solution and the Newtonian glycerol-solution for similar Weber numbers. This diameter enlargement also occurs at the subsequent collision complex oscillations.

The dimensionless time for the build-up of the collision complex maximum expansion is independent from viscosity characteristics; it is only a function of the Weber number. Hence, the absolute time for reaching maximum complex diameter for a given *We* is merely proportional to the ratio of droplet diameter to droplet velocity.

The same droplet morphologies are found by simulation and experiment. This result shows that the used description of the test fluid behaviour by the generalized Newtonian model is appropriate for the given flow situation. It verifies the code's ability to simulate two-phase flow for this class of non-Newtonian fluids. The simulation gives correct results for the surface shapes and sizes. The time scale of the collision complex contraction is overestimated; an effect, which also occurs for Newtonian calculations.

Simulated velocity fields show that, at all stages of the collision process, areas exist, in which the velocity gradients for shear are larger than the elongational ones, and vice versa. Overall, elongational flow dominates.

The simulated viscosity field shows that during the collision only lowered values of viscosity occur. This suggests a greater similarity between Newtonian and non-Newtonian flows with equal high-shear viscosities instead of flows with equal zero-shear viscosities. Therefore, a natural question to be addressed in the future is, if there is a kind of equivalent Newtonian droplet collision based on modified dimensionless groups.

Nomenclature

d	collision complex diameter
d_P	distance of planes in channel flow
D	droplet diameter before impact
K	fluid consistency index of viscosity model
L	pressure loss length in channel flow
n	flow index of viscosity model
Re	Reynolds Number, $Re = Ud\rho/\mu_0$
Re_M	modified Reynolds Number, $Re_M = U^2\rho/(\dot{\gamma}\ \mu_0)$
t	time
t^*	dimensionless time, $t^* = t/(D/U)$
u	velocity vector
U	relative collision velocity
v	fluid velocity of channel flow
We	Weber Number, $We = U^2D\rho/\sigma$
y	coordinate normal to planes in channel flow
$\dot{\gamma}$	shear rate
ΔP	pressure loss over L in channel flow
μ	dynamic viscosity
μ_0	dynamic zero shear rate viscosity
μ_N	Newtonian dynamic viscosity
$\bar{\mu}$	elongational viscosity
ρ	density of liquid
σ	surface tension
τ	deviatoric stress tensor

References

[1] Roth, N., Rieber, M., and Frohn, A., "High energy head-on collisions of droplets", *Fifteenth International Conference on Liquid Atomization and Spray System*s, Toulouse, France, July 1999.

[2] Frohn, A., Roth, N., *Dynamics of Droplets*, Springer, 2000, p. 66.

[3] Hirt, C.W., Nichols, B.D., "Volume of Fluid (VOF) Method for the Dynamics of Free Boundaries", *Journal of Computational Physics* 39, 201-225, (1981).

[4] Rieber, M., Frohn, A., "A numerical study on the mechanism of splashing", *Int. J. Heat and Fluid Flow* 20, 455-461, (1999).

[5] Bird, R.B., Armstrong, R.C., Hassager, O., *Dynamics of Polymeric Liquids*, V. 1, Wiley-Interscience, 1987, pp. 169-253.

[6] Lafaurie, B., Nardone, C., Scardovelli, R., Zaleski, S., and Zanetti, G., "Modelling merging and fragmentation in multiphase flows with SURFER", *J. Comp. Phys.*, 113, 134-147, (1994).